Supplementary Information (SI) for RSC Applied Polymers. This journal is © The Royal Society of Chemistry 2026

Electronic Supplementary Information (ESI)

Mechanical Properties of Individual Conductive Protein Nanowires and Their Percolation Behavior in Elastomer Nanocomposites

Eric Chia,[a] Jayesh M. Sonawane,[b] Trevor L. Woodard,[c] Meng-Chen Chiang,[d] Jessica D. Schiffman,[d,e] and Stephen S. Nonnenmann[a,e*]

[a]Department of Mechanical and Industrial Engineering, University of Massachusetts Amherst, 686 N Pleasant St., Amherst, MA 01003, USA

[b]Department of Microbiology, Central University of Rajasthan, Ajmer 305817, Rajasthan, India

[c]Department of Microbiology, University of Massachusetts Amherst, 639 N Pleasant St., Amherst, MA 01003, USA

[d]Department of Chemical and Biomolecular Engineering, University of Massachusetts Amherst, Amherst, MA 01003, USA

[e]Materials Science and Engineering Graduate Program, University of Massachusetts Amherst, Amherst, MA 01003, USA

*Corresponding author: Stephen S. Nonnenmann; Email: ssn@umass.edu

---

1 Persistence Length of CPN, CNT and AgNW

The greater the persistence length of nanofiller, the more volume that it could interact with substrate. The persistence length, L_p is defined as:

$$L_p = \frac{EI}{k_B T} \tag{S1}$$

where E is the Young's modulus, I is the area moment of inertia, k_B is the Boltzmann's constant and T is the temperature. The moment of inertia of rod-like nanofillers could be simplified as:

$$I = \frac{\pi(d_{outer}^4 - d_{inner}^4)}{64} \tag{S2}$$

where d is the diameter of nanofillers. By substituting the information of CPN measured by AFM, with $d_{CPN} = 3$ nm and $E_{CPN} = 1.3$ GPa, the $L_{p,CPN} = 1.25$ µm. Comparing to AgNW by assuming the $d_{AgNW} = 65$ nm and $E_{AgNW} = 86.5$ GPa[1], the $L_{p,AgNW} = 18.3$ m; for CNT, substituting the $d_{outer} = 5.6$ nm, $d_{inner} = 2.3$ nm and $E_{CNT} = 1$ TPa[2], the $L_{p,CNT} = 0.01$ m. These persistence length calculations have proven that CPN have shorter persistence length, which means they tend to bend and curl. The calculation of CPN persistence length is similar to the observation of type IV pili of *Pseudomonas Aeruginosa*, which also has the persistence length of approximately 1 µm under AFM[3]. The substantially shorter persistence length of CPNs relative to CNTs and AgNWs informs their tendency to form bundles in organic media, which is discussed in the context of filler-matrix interactions and percolation behavior in Section 3.3 of the main text.

2 Topographic Height and Modulus Line Profiles

Figure S1 provides the height and Young's modulus line profiles extracted along a single CPN from the fast force mapping (FFM) data described in Section 3.1, illustrating the spatial correlation between nanowire topography and local mechanical response that underpins the reported modulus of 1.3 ± 0.1 GPa.

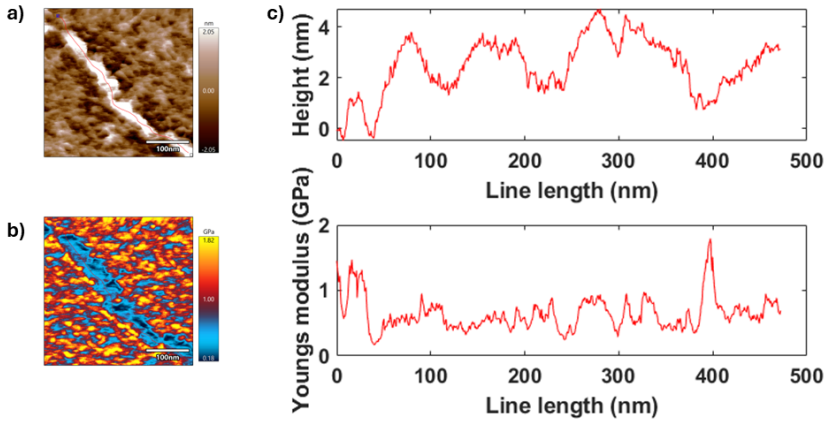

Figure S1. The process of analysis height and corresponding Young's modulus of single CPN acquired by FFM. a shows the height of CPN and b shows the corresponding Young's modulus. The red curve depicted on a and b are plotted on c that shows the height and Young's modulus of CPN.

3 AM-FM Bimodal Modulus Imaging by Filler Content

Figure S2 shows AM-FM Young's modulus maps of CPNs/PDMS composites across all filler loadings from 0 to 10 wt%, providing the spatial context for the modulus values plotted in Figure 4a of the main text and confirming the progressive mechanical reinforcement of the matrix with increasing CPN concentration.

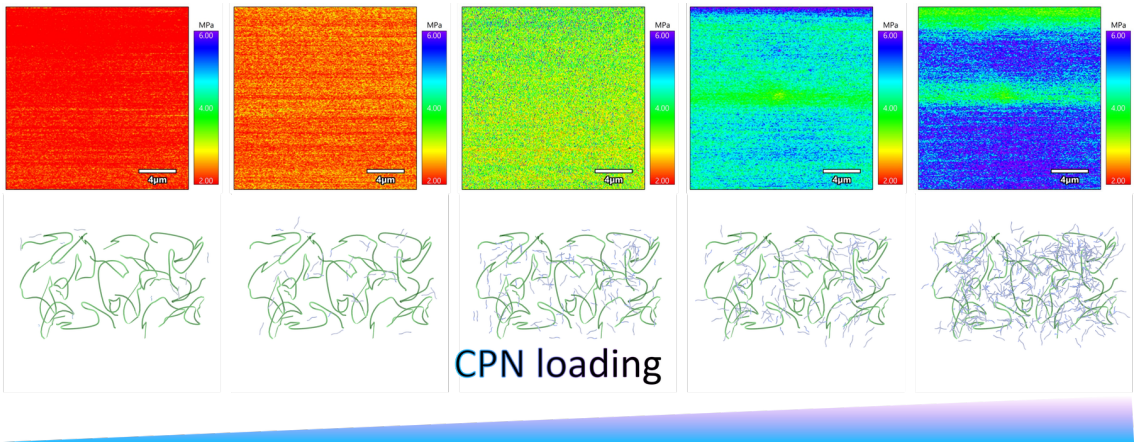

Figure S2. Elaboration on Young's modulus measurements of CPNs/PDMS by using AM-FM AFM. Starting from left is the pure PDMS and then 1, 2, 5, and 10 wt% CPNs/PDMS.

4 I-V Measurements of Pure and CPN-PDMS Systems

Figure S3 shows representative I-V curves measured above (7 wt%) and below (6 wt%) the electrical percolation threshold, demonstrating the sharp contrast in current response at the onset of electrical conductivity discussed in Section 3.3 of the main text.

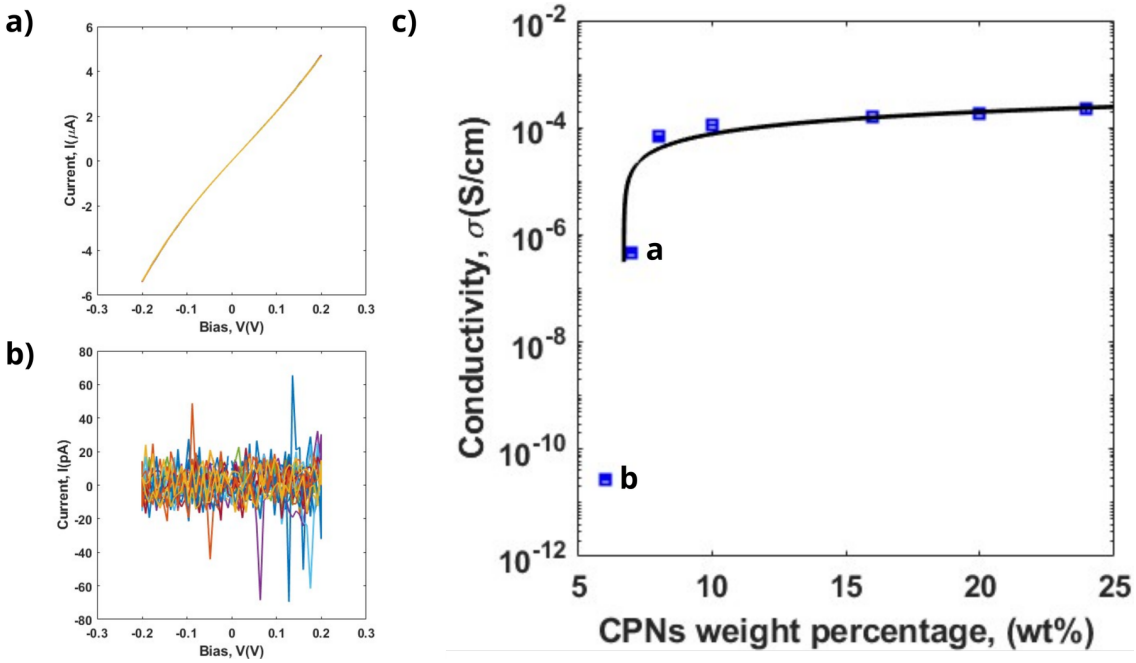

Figure S3. The representative I-V curves of CPNs/PDMS. a) is the I-V curves of 7 wt% that shows resistance response of CPNs/PDMS, while b) shows the I-V curves of 6 wt% that shows little or no current flowing through the samples that below the detection limits of Keithley 2401. b) is the iconic I-V curves that is below the electrical percolation threshold. c) shows the electrical conductivity (S/cm) as a function of CPNs weight percentage, illustrating the percolation behavior across the full loading range measured.

5 Radius of Gyration of Dow Sylgard 184 PDMS Chain

The material safety data sheet (MSDS) for Dow Sylgard 184 reports a bulk dynamic viscosity of 3500 cP. This value represents the viscosity of the pure, undiluted "Part A" resin as supplied, describing the macroscopic entanglement of polymer chains rather than their hydrodynamic behavior in a solvent. Even if bulk viscosity correlations (where $\eta_0 \propto M_w^{3.4}$) were applied to estimate the molecular weight, relying on the 3500 cP value from the datasheet is misleading. Sylgard 184 is not purely composed of polydimethylsiloxane (PDMS); the base resin contains a significant mass fraction (often 30–40% by weight) of fumed silica nanoparticles incorporated to reinforce the cured silicone. These solid particulate fillers artificially inflate the bulk viscosity. Because Dow Sylgard 184 is a proprietary commercial formulation rather than a pure analytical standard, characterizing its exact molecular weight remains a well-documented challenge in materials science and membrane research.

A definitive study characterizing the uncrosslinked components of Sylgard 184 was conducted previously by utilizing gel permeation chromatography (GPC), and the molecular weight distributions of both the pre-polymer (Part A) and the cross-linker (Part B) are determined.[4] A crucial finding was that the Sylgard 184 Part A pre-polymer lacks a single, uniform chain length. Instead, the data revealed a bimodal molecular weight distribution comprising two primary polymer chain populations: a low-molecular-weight fraction of approximately 4000 g/mol and a high-molecular-weight fraction of approximately 67000 g/mol. This bimodal nature elucidates why estimating a singular average molecular weight from the bulk dynamic viscosity (3500–4000 cP) is fundamentally impractical; the macroscopic viscosity is a physical amalgamation of the short chains, the long chains, and the dense silica reinforcement. Consequently, to acquire accurate molecular measurements, the resin cannot be tested in its as-supplied state. The pure polymer must first be extracted from the silica fillers.

To estimate the root-mean-square radius of gyration (R_g) for a PDMS chain with a molecular weight of 67000 g/mol, two distinct polymer physics frameworks can be applied depending on the environment: first-principles chain statistics (for an unperturbed coil in a theta solvent such as MEK or in the bulk melt) and hydrodynamic scaling (for a swollen coil in a good solvent such as toluene). The detailed estimations for both thermodynamic scenarios are provided below.

5.1 The "Unperturbed" R_g (In MEK or Bulk Melt)

In a theta solvent (MEK at 25°C) or within the pure bulk state prior to cross-linking, the PDMS chain behaves as an "ideal" random coil. The R_g can be calculated utilizing the Flory characteristic ratio (C_∞), which accounts for the bond angles and steric hindrances inherent to the polymer backbone.

Step 1: Define the molecular parameters for PDMS

Monomer unit: $[-Si(CH_3)_2O-]$

Monomer molecular weight (M_0): 74.15 g/mol

Average backbone bond length (l): The Si–O bond is exceptionally flexible and long, averaging 1.64 Å (0.164 nm).

Characteristic ratio (C_∞): Because PDMS is highly flexible, it has a low C_∞, typically taken as 6.2 at room temperature.

Step 2: Calculate the number of backbone bonds (n)

First, the degree of polymerization (N) is determined:

$$N = \frac{M}{M_0} = \frac{67000}{74.15} \approx 903.6 \text{ repeat units} \tag{S3}$$

Since each repeat unit has two backbone bonds (Si–O and O–Si), the total number of bonds is:

$$n = 2N \approx 1{,}807 \text{ bonds} \tag{S4}$$

Step 3: Calculate the unperturbed end-to-end distance ($\sqrt{\langle r^2 \rangle_0}$)

$$\langle r^2 \rangle_0 = C_\infty n l^2 \tag{S5}$$

$$\langle r^2 \rangle_0 = 6.2 \times 1807 \times (1.64)^2 \approx 30132 \text{ Å}^2 \tag{S6}$$

$$\sqrt{\langle r^2 \rangle_0} = \sqrt{30132} \approx 173.6 \text{ Å } (17.36 \text{ nm}) \tag{S7}$$

Step 4: Calculate R_g

For an ideal linear polymer, the radius of gyration is geometrically related to the end-to-end distance by a factor of $1/\sqrt{6}$:

$$R_{g,\theta} = \frac{\sqrt{\langle r^2 \rangle_0}}{\sqrt{6}} = \frac{173.6}{\sqrt{6}} \approx 70.8 \text{ Å} \tag{S8}$$

Yielding an unperturbed $R_g \approx 7.08$ nm.

5.2 The "Swollen" R_g (In a Good Solvent like Toluene)

When dissolving this 67,000 g/mol chain fraction in toluene, favorable polymer-solvent interactions cause the coil to expand due to excluded volume effects. This swollen R_g can be estimated using the Flory-Fox equation, which correlates the intrinsic viscosity ($[\eta]$) with the hydrodynamic volume.

Step 1: Calculate intrinsic viscosity in Toluene

Using the Mark-Houwink parameters for PDMS in Toluene ($K = 0.020$, $a = 0.66$):

$$[\eta] = 0.020 \times (67000)^{0.66} \approx 29.2 \text{ mL/g} \tag{S9}$$

Step 2: Apply the Flory-Fox Equation

The universal relationship between $[\eta]$ and R_g is:

$$[\eta] = \Phi' \frac{R_g^3}{M} \tag{S10}$$

Where Φ' is the Flory viscosity constant. When $[\eta]$ is expressed in mL/g and R_g in cm, $\Phi' \approx 4.29 \times 10^{24}$ mol^{-1}. Rearranging the equation to solve for R_g^3:

$$R_g^3 = \frac{[\eta]M}{\Phi'} = \frac{29.2 \times 67000}{4.29 \times 10^{24}} \approx 4.56 \times 10^{-19} \text{ cm}^3 \tag{S11}$$

Step 3: Calculate the expanded R_g

$$R_g = (4.56 \times 10^{-19})^{1/3} \approx 7.69 \times 10^{-7} \text{ cm} \tag{S12}$$

Yielding a swollen $R_g \approx 7.69$ nm.

In conclusion, verifying a definitive radius of gyration (R_g) for Sylgard 184 is challenging due to its polydisperse composition of PDMS chains. These estimates confirm that the R_g of the higher molecular weight PDMS chains in Sylgard 184 exceeds the critical inter-particle distance required for electron transport, consistent with the rheological percolation threshold occurring at lower filler loading than the electrical threshold in the CPN/PDMS system.

Figure S4 shows the I-V curve of a pristine PDMS-infiltrated AAO template with no CPNs present, confirming that the template itself contributes no measurable electrical conductivity prior to CPN infiltration and that the conductivity enhancements reported in Section 3.4 of the main text originate exclusively from the CPN filler network.

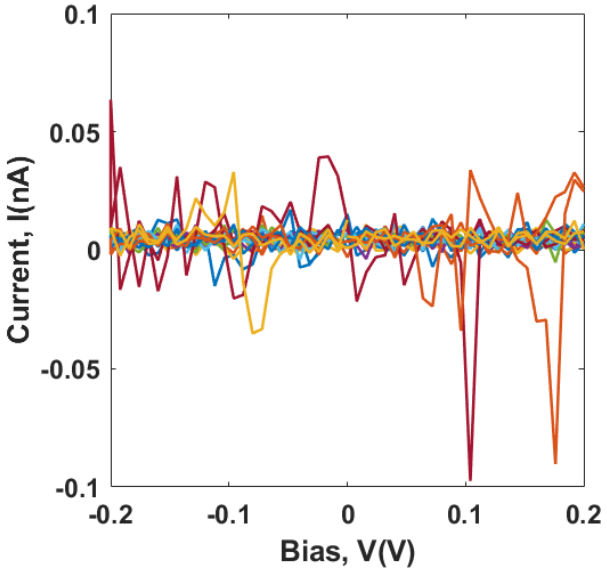

Figure S4. The IV curve of pristine PDMS infiltrated in AAO template. The conductivity is 2.17×10^{-11} S/cm, which is beyond the measuring scope of the sourcemeter, indicating the insulating behavior.

6 CPNs/PDMS Based Strain Sensors: A Pilot Application

After establishing the functional properties of the CPNs/PDMS nanocomposites, the focus shifted to efforts that demonstrate potential scalability and viability of applied systems, where a strain gauge was selected as the pilot study. To fabricate nanocomposite dog-bone structures capable of withstanding both tensile loads and simultaneous electrical measurements, the base CPN solution concentration was scaled from 90 µg/µL to 675 µg/µL. Additionally, the sample volume was increased threefold compared to the spin-coated samples deposited on the interdigitated electrode setups to ensure sufficient mechanical integrity for electrode wiring and loading. Figure S5a shows the schematic diagram of the dog-bone elongation experiment and the linear response between resistance variations and applied strain (max 50%) is plotted in Figure S5b. The average gauge factor is 0.47, lower than typical commercial strain gauge values (k = 2–5). As a pilot test structure comprising significantly higher CPNs volumes, these basic strain sensors exhibit the expected

linear response; however, further studies on scaled dispersion and electrical threshold enhancement will be necessary to optimize CPNs/PDMS nanocomposite-based sensors, and are currently outside the scope of this study.

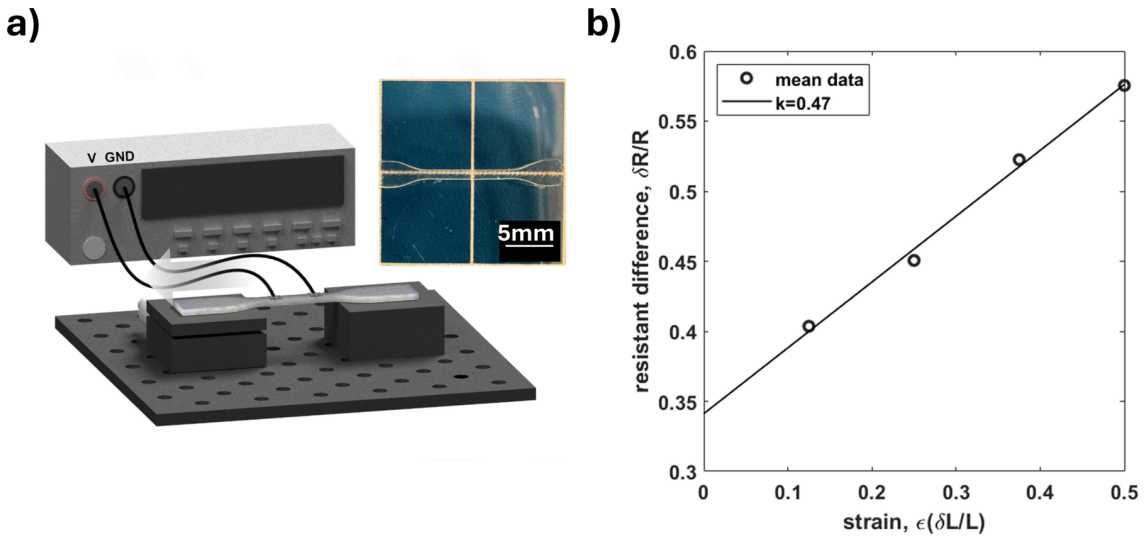

Figure S5. a) shows the schematic diagram of 20 wt% CPNs/PDMS dog-bone elongation experiments. The inset is the translucent dog-bone for experiments. The resistance response with respect to strain is plotted in b). Both show a linear response between resistance and strain, and can be potentially utilized as a highly flexible strain gauge.

References

[1] Y. Chen, B. L. Dorgan, Jr., D. N. McIlroy and D. Eric Aston, *Journal of Applied Physics*, 2006, **100**, 104301.

[2] M. M. J. Treacy, T. W. Ebbesen and J. M. Gibson, *Nature*, 1996, **381**, 678–680.

[3] S. Lu, A. Touhami, H. Harvey, E. Scheurwater, L. Burrows and J. R. Dutcher, *Biophysical Journal*, 2009, **96**, 641a–642a.

[4] N. Stafie, D. Stamatialis and M. Wessling, *Separation and Purification Technology*, 2005, **45**, 220–231.